Thermodynamic Study of Compartment Venting

Francisco Manuel Bargado Benavente
francisco.benavente@tecnico.ulisboa.pt
Instituto Superior Técnico, Universidade de Lisboa
Lisbon, Portugal

Abstract **–** *Compartment venting, among others, is one of the most important criteria in the construction of space-vehicles. This paper presents an analytical model that can forecast the pressure evolution of a single compartment. To validate the results obtained, a laboratory experiment was performed. Two case studies were analysed: a compressed tank and the spacecraft scenario, in which the atmospheric pressure decreases over time. The paper also provides an one-dimensional analytical model and a two-dimensional numerical model, which was performed by SolidWorks add-in Flow Simulation. Most results of the developed analysis are presented herein.*

Keywords: Compartment venting, analytical model, numerical analysis, pressure evolution

I. INTRODUCTION

The race for space exploration started around 1940, and the Russian satellite Sputnik was the first spacecraft developed [1]. Afterwards, several issues that can provoke accidents have been related to excessive pressure differential between the space-vehicles compartments. As a launch vehicle ascends, the air contained within compartments must be vented overboard to a decreasing atmospheric pressure. If venting is not efficient, the walls of the compartment may be subjected to critical loads due to the pressure differential. The sudden failure of upper stage insulation panels has been attributed to improper venting. Boxes for electronic equipment have exploded, honeycomb sandwich structures have also failed by delamination from bursting pressures caused by entrapped air. Engine failures have also been related to improper venting [2]. Venting, or depressurization, has also been discussed as a possible technique for extinguishing fires on aircrafts and spacecrafts [3].
For instance, a complete launch vehicle failed by a problem venting in the heat shields. The vents flow will also influence the outer flow and can degrade the aerodynamic properties of the spacecraft [4].
The vent sizing problem is complex, since the vents need to consider compartment geometry, equipment, temperature, compartment interconnections, contaminations, etc. The location and distribution of the vents also needs to be calculated, in order to maintain the aerodynamic characteristics of the space-vehicle [2]. Vents can be classified into general categories of orifices, valves, tubes, pipes or ducts and porous materials. Each type of vent leads to different flow behaviours [2].
Compartment venting is one the most important criteria in the construction of space-vehicles. Over time, several fast and simple models have been developed to forecast the highest pressure differential between the walls of a single and simple geometry compartment.
The main goal of this work is to present a novel model that can forecast the pressure evolution of a single compartment. Results also include a laboratory experiment and a numerical analysis of the compartment flow.

II. ANALYTICAL ANALYSIS OF THE COMPARTMENT FLOW

The present analytical model considers a non-steady one-dimensional isentropic flow of a perfect gas.
Through a mass balance and using the perfect gas equation:

$$\frac{V}{R}\frac{d}{dt}\left(\frac{P}{T}\right) = -\rho_e A_v u_e \tag{2.1}$$

Assuming no internal irreversibilities and adiabatic flow, the isentropic relations can be used [5]. Equation (2.1) is simplified:

$$u_e = -\frac{V}{\gamma A_v P_{ext}}\frac{dP}{dt} \tag{2.2}$$

Using a mass balance to determine the function $u(x)$ and the isentropic relations, the non-steady Bernoulli equation becomes:

$$\frac{G}{\gamma}\frac{d^2 \ln P}{dt^2} - \left(\frac{V}{\sqrt{2}\gamma P_e A_v}\right)^2 \left(\frac{dP}{dt}\right)^2 + \frac{P - P_e}{\rho_0}\left(\frac{P_0}{P}\right)^{\frac{1}{\gamma}} = 0 \tag{2.3}$$

in which: $G = \int_0^L \frac{V(x)}{A(x)} dx$.

The Mach number at the exit section cannot be greater than 1, therefore an iterative process is needed to solve Equation (2.3). If the Mach number is greater than 1, the exterior pressure needs to be slightly increased in order to obtain sonic conditions.

A. Solution method

As the problem is unconditionally unstable, the solution was obtained using the finite difference method. The derivatives are approximated and Equation (2.3) is rewritten as:

$$\frac{P_{j+1} - 2P_j + P_{j-1}}{h^2} - \left(\frac{1}{P_j} + \frac{\gamma a^2 P_j}{G}\right)\left(\frac{P_{j+1} - P_{j-1}}{2h}\right)^2 + \frac{\gamma b^2}{G}\frac{P_j^2 - P_j P_e}{P_j^{\frac{1}{\gamma}}} = 0 \tag{2.4}$$

in which: $a = \frac{V}{\sqrt{2}\gamma P_b A_e}$ and $b = \sqrt{\frac{P_0^{\frac{1}{\gamma}}}{\rho_0}}$.

However, the first iteration needs to be calculated through another method. The finite difference method requires the known of P_2 and P_1 (initial pressure) in order to determine P_3. In order to maintain the convergence order, the fourth order Runge-Kutta method is used. The software Mathematica was used to solve Equation (2.5) through the Newton Method to determine P_{j+1} in each iteration.

B. Dimensionless Analysis

The dimensionless analysis is performed to determine a dimensionless solution which can be used for similar flows. By the adimensionalization of each variable, Equation (2.2) and Equation (2.3) are written, dimensionless, as:

$$u_e^* = -\frac{VP_0}{\gamma P_e A_v L}\frac{dP^*}{dt^*} \tag{2.5}$$

$$\frac{G}{L^2}\frac{d^2 \ln P^*}{dt^{*2}} - \left(\frac{VP_0}{\sqrt{2}\gamma P_e A_v L}\right)^2 \left(\frac{dP^*}{dt^*}\right)^2 + \frac{P^* - P_e^*}{P^{*\frac{1}{\gamma}}} = 0 \tag{2.6}$$

From Equation (2.5) and Equation (2.6), three dimensionless groups are identified, however the two major dimensionless groups are: $G_1 = \frac{G}{L^2}$ and $G_3 = \frac{VP_0}{\gamma P_e A_v L}$. The dimensionless results for both case studies are shown in [6].

III. NUMERICAL ANALYSIS OF THE COMPARTMENT FLOW

For the one-dimensional analysis, an Arakawa-C grid was applied. For this staggered grid, the density and pressure are calculated at the center of the cell and the velocity components are calculated at the center of the grid faces. Inviscid flow is considered to simplify the analysis.

A. Formulation

The Euler equation is used in the conservative form. Assuming an isothermal system and using the continuity equation and the perfect gas law, an equation for the pressure is calculated. The equations' system to solve the problem is:

$$p = \rho RT \tag{3.1}$$

$$\frac{\partial \rho u}{\partial t} + \frac{\partial \rho u u}{\partial x} = -\frac{\partial P}{\partial x} \tag{3.2}$$

$$\frac{\partial P}{\partial t} + \frac{\partial P u}{\partial x} = 0 \tag{3.3}$$

The equations were discretized using the finite difference method, except the advective term in Equation (3.2) that was discretized using an upwind scheme. Due to numerical diffusion and errors resulting from

the discretization, the pressure at the exit can decrease below the atmospheric pressure which is physically not possible. To overcome this issue, a pressure condition must be stated: if $P_e(t) \leq P_b$, then $P_e(t) = P_b$.

B. *Solution methods*

i. Explicit method

Using the explicit method, the system of equations to be solved is:

$$\frac{(\rho u)^{t+1} - (\rho u)^t}{\Delta t} + \frac{\partial (\rho u u)^t}{\partial x} = -\left(\frac{\partial P}{\partial x}\right)^t \tag{3.4}$$

$$(Pu)^{t+1} = RT(\rho u)^{t+1} \tag{3.5}$$

$$\frac{P^{t+1} - P^t}{\Delta t} + \left(\frac{\partial Pu}{\partial x}\right)^{t+1} = 0 \tag{3.6}$$

To solve the system, the vector $(\rho u)^{t+1}$ is determined from Equation (3.4). From Equation (3.5), the vector $(Pu)^{t+1}$ is calculated. The pressure in each cell is determined by Equation (3.6) (the density is calculated using the perfect gas law).
To ensure the stability of the explicit method, the Courant-Friedrichs-Lewy condition must be satisfied. In one-dimensional transient problems the condition is stated as: $C = \frac{u\,\Delta t}{\Delta x} \leq 1$.

ii. Crank-Nicolson method

For this method, the Euler equation is modified, as the pressure gradient is discretized using the Crank-Nicolson scheme. The second order derivative is approximated using the central finite difference method. Equation (3.4) is rewritten as:

$$\frac{(\rho u)^{t+1} - (\rho u)^t}{\Delta t} + \frac{\partial (\rho u u)^t}{\partial x} = -\frac{1}{2}\left[-RT\Delta t\left(\frac{\partial^2 \rho u}{\partial x^2}\right)^{t+1} + 2\left(\frac{\partial P}{\partial x}\right)^t\right] \tag{3.7}$$

Equation (3.7) is solved through a tri-diagonal matrix. The vector (ρu) is determined from Equation (3.7). The velocity, pressure and density are determined as in the explicit method. The Crank-Nicolson method is unconditionally stable although it may have numerical diffusion [7].

IV. LABORATORY EXPERIMENT

A. *Compressed tank case study*

The objective of this experiment is to record the internal pressure evolution for different initial pressures and venting areas. A cylindrical stainless steel tank with a length of 880 mm and a diameter of 350 mm was used to perform the experiment. Each venting areas, with the diameters of 5 and 2 mm, were tested for the initial pressures of 2, 3 and 4 bar. The experiment is shown in Figure 1.

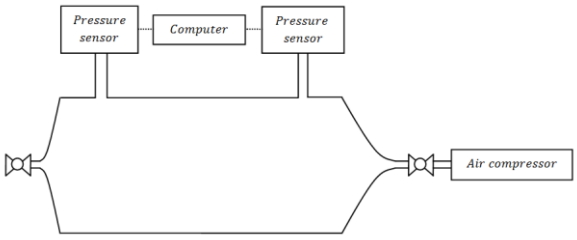

Figure 1 - Experimental installation of the compressed tank case study.

Two sensors were used to record the pressure, in order to determine the average tank pressure. The sensors were connected to an Arduino Uno. The sensors uncertainty is known and it is calculated by:

$$S = \pm\frac{0.25 + 0.03}{100}4 = \pm\, 0.0112\ bar$$

B. *Spacecraft case study*

For this experiment, an additional tank was used. The Pyrex glass tank has a length of 200 mm and a diameter of 100 mm. The Pyrex tank simulates a spacecraft compartment and the steel tank simulates the atmosphere, with a decreasingly pressure. To decrease the pressure in the steel tank, a vacuum pump and a commercial vacuum cleaner were used. To test different venting areas, the connection between both tanks was carried out using hoses with diameters of 5, 2 and 1 mm. Two sensors were also needed for this experiment, one for each tank. The experimental installation is shown in Figure 2.

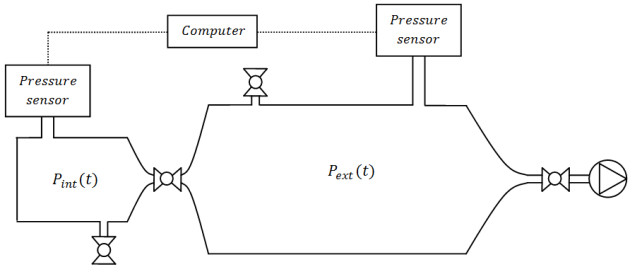

Figure 2 - Experimental installation of the spacecraft case study.

Concerning the use of the vacuum pump, since the Pyrex glass only has a thickness of 3 mm, the experiment could only be performed until the pressure of 0.7 bar is reached. However, the vacuum cleaner can only decrease the pressure to approximately 0.81 bar.
The pressure curve of the steel tank was used in the models to compare the results recorded from the experiment to those obtained from the developed methods.

V. RESULTS AND DISCUSSION

A. *Laboratory experiment*

For the compressed tank case study, Figure 3 shows the recorded pressure evolutions.

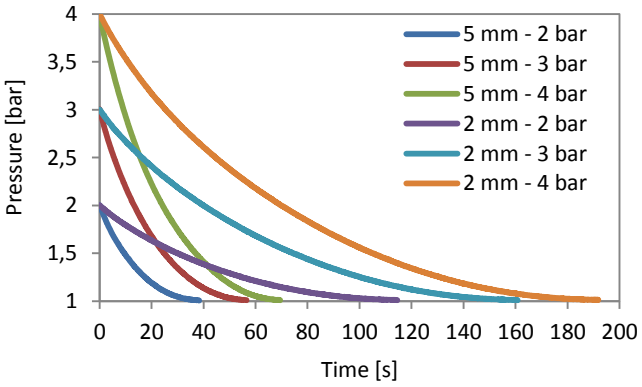

Figure 3 - Pressure evolutions obtained in the laboratory experiment for the compressed tank case study.

Table 1 shows the time required to resettle atmospheric conditions for each nozzle diameter and initial pressures.

Table 1 - Time (s) required to resettle atmospheric conditions.

Initial pressure (bar)	**φ: 5 mm**	**φ: 2 mm**
2	38.3	114.5
3	56.5	160.8
4	69.5	191.9

Figure 4 shows the pressure evolutions of both tanks for each connection diameter, for the spacecraft case study and using the vacuum pump to decrease the steel tank pressure.

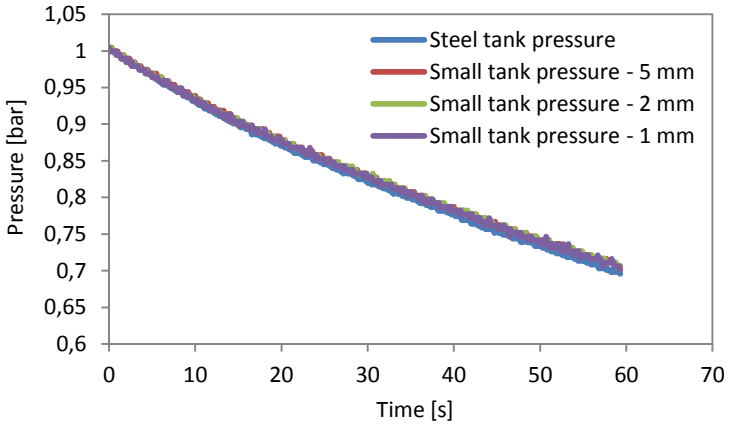

Figure 4 - Pressure evolution of both tanks for the vacuum pump.

The vacuum pump takes, approximately, a minute to decrease the atmospheric pressure to 0.7 bar. Therefore, all venting areas are efficient as the compartment pressure is approximately equal to the steel tank pressure. The vacuum pump leads to a slow pressure decay rate. However, for the vacuum cleaner, Figure 5 shows the pressure evolution of both tanks.

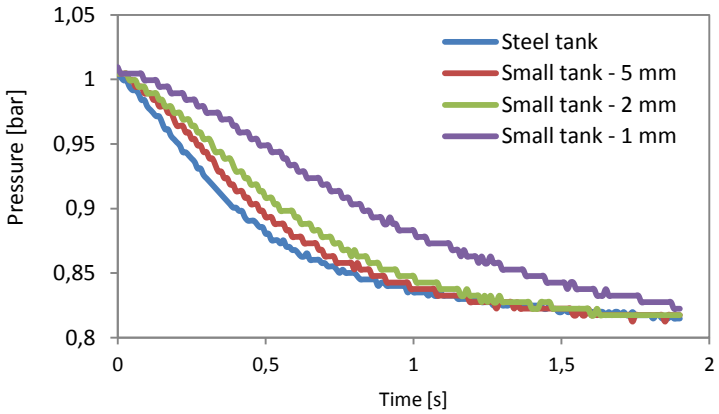

Figure 5 - Pressure evolution of both tanks for the vacuum cleaner.

The vacuum cleaner decreases the atmospheric pressure to 0.81 bar in 1.9 seconds. As the venting area becomes smaller, the pressure differential increases. The maximum pressure differential detected was 0.0707 bar at 0.55 seconds, when the smallest nozzle was used.

B. Numerical analysis of the compartment flow

i. One-dimensional model

For the one-dimensional analysis, the venting area cannot be defined, as a change in the cross section implies at least a 2D model. For the Crank-Nicolson method, a numerical time step of 0.0001 s was defined. The model features 880 cells, each with a length of 1 mm. For the explicit method, in order to satisfy the Courant-Friedrichs-Lewy condition, a numerical time step of 0.000025 s was defined. Figure 6 shows the pressure evolution obtained from both methods for each initial pressure.

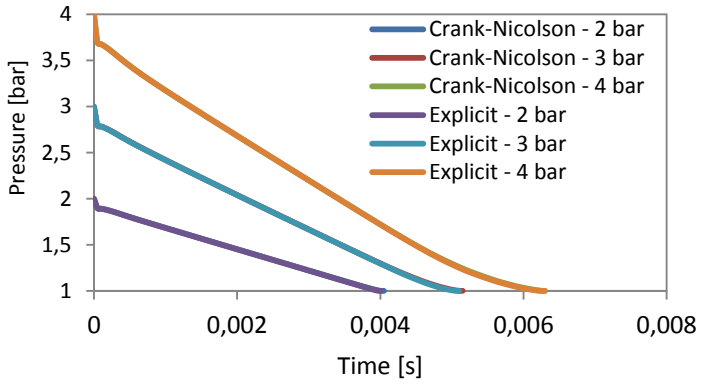

Figure 6 - Pressure evolution obtained for both 1D methods and initial pressure.

Table 2 shows the time required to resettle atmospheric conditions for both methods and initial pressures.

Table 2 - Time (s) required to resettle atmospheric conditions for both 1D methods and initial pressure

Initial pressure (bar)	Explicit method	Crank-Nicolson method
2	0.004	0.00405
3	0.0051	0.00515
4	0.0063	0.0063

For the spacecraft case study, Figure 7 shows the results for the compartment pressure.

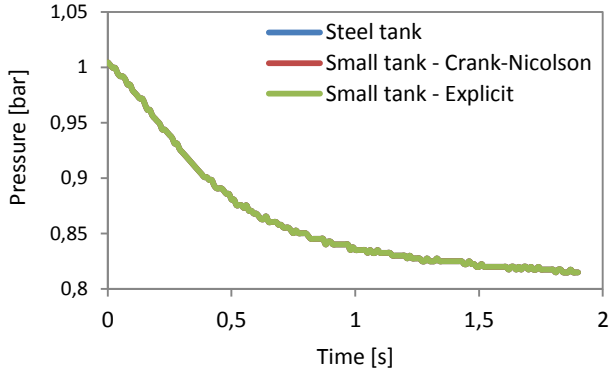

Figure 7 - Pressure evolution of both tanks obtained from both 1D methods.

The one-dimensional model yields an extremely fast process. The times to resettle atmospheric conditions, for the compressed tank case study, are very small when compared to the data obtained from the experiment. Regarding the spacecraft case study, no pressure differential is detected. For both methods, the compartment pressure is always equal to the steel tank pressure. For the first case study, the explicit method presents a slightly bigger decay rate and atmospheric conditions are reached faster than in the Crank-Nicolson method. The one-dimensional model simulates a tank with constant cross section area, i.e., a pipe with constant diameter, which leads to faster processes. For the used geometry, the model is not suitable, however the one-dimensional analysis should provide accurate results when vents such as ducts, pipes or tubes are used.

ii. Two-dimensional model

The two-dimensional analysis was performed by SolidWorks add-in Flow Simulation. For the compressed tank case study, the steel tank was modeled and features 610382 fluid cells and 51050 partial cells. Figure 8 shows all the pressure evolutions for the 5 mm nozzle and each initial pressure.

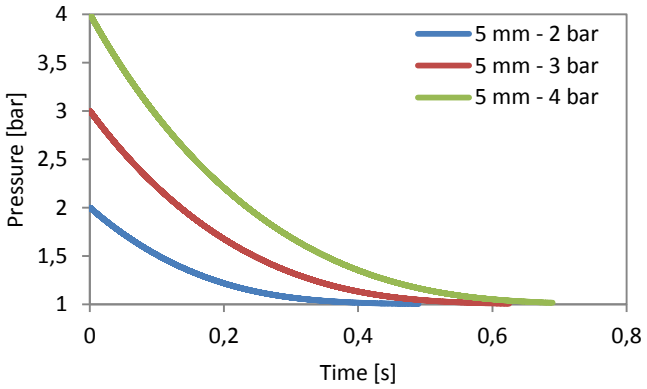

Figure 8 - Pressure evolution of the steel tank for each initial pressure obtained through the 2D model.

Table 3 shows the times required to achieve atmospheric conditions for each initial pressure.

Table 3 - Time (s) required to achieve atmospheric pressure through the 2D model.

Initial pressure (bar)	**Time**
2	0.49
3	0.625
4	0.735

Regarding the spacecraft case study, the smaller tank was modeled in SolidWorks. The tank features 13934 partial cells and 102310 fluid cells. Figure 9 shows all the pressure evolutions for each nozzle diameter.

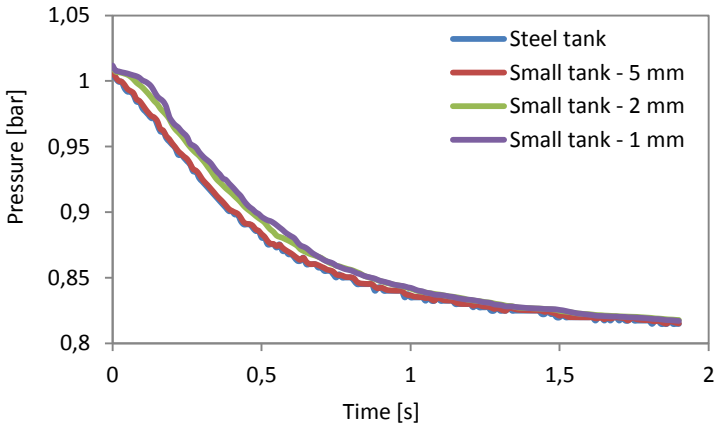

Figure 9 - Pressure evolution of both tanks for each connection diameter obtained from the 2D model.

The relevant direction of the flow is along x, but for a three-dimensional model the continuity equation shows that the order of magnitude of $\partial v/\partial y$ is similar to the order of magnitude of $\partial w/\partial z$. Assuming that the flow is axisymmetric, this implies that the length scale along z is similar to the length scale along y, $L_y \approx L_z$. However the numerical grid used for the two-dimensional model only considers a grid cell in the z direction, which is the same as assuming that $\partial/\partial z = 0$, i.e., $L_z \gg L_y$. This is obviously wrong for the case of the geometry considered in this work, which means that a three-dimensional model should have been used instead of the two-dimensional model. Computational limitations, however, explain the choice made.

The two-dimensional process also yields a fast process, since the model does not consider the velocity component along the z-axis and the wall effect. For the compressed tank case study, the time required to achieve atmospheric conditions from the initial pressures is very small when compared to the data recorded from the laboratory experiment. Regarding the spacecraft case study, the pressure differentials detected are smaller than those obtained from the experiment.

C. Analytical analysis of the compartment flow

Using a numerical time step of 0.001 s, Figure 10 shows the pressure evolutions for each nozzle diameter and initial pressure.

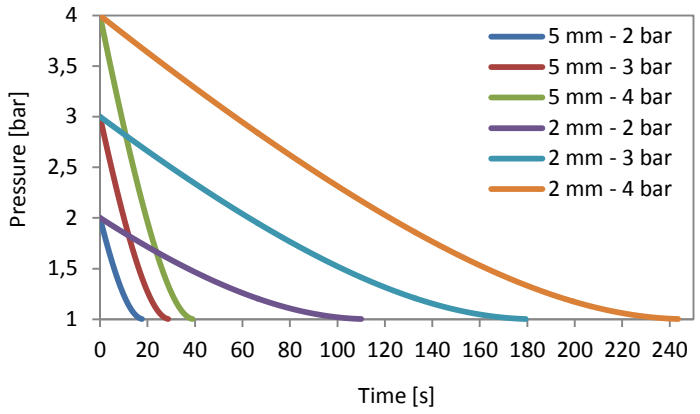

Figure 10 - Pressure evolutions obtained through the analytical model for each nozzle diameter and initial pressure.

Table 4 shows the time required to resettle atmospheric conditions for each nozzle diameter and initial pressure.

Table 4 - Time (s) required to resettle atmospheric conditions for the analytical model

Initial pressure (bar)	**φ: 5 mm**	**φ: 2 mm**
2	17.6	110
3	28.7	179.3
4	39	243.6

Regarding the spacecraft case study, Figure 11 shows the evolutions of both tanks for each diameter.

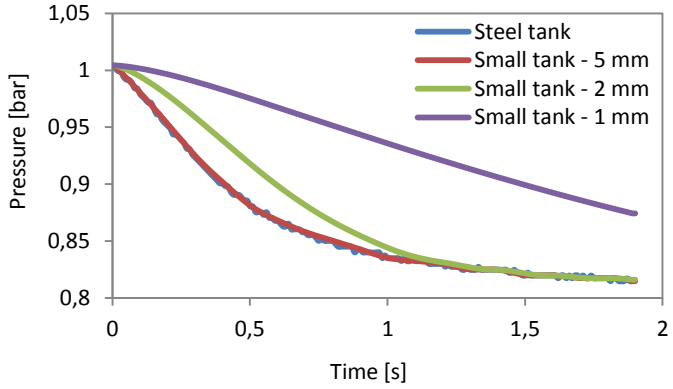

Figure 11 - Pressure evolution of both tanks for each nozzle diameter obtained through the analytical model.

For the compressed tank case study, the times to resettle atmospheric conditions from the analytical model and the experiment have the same order of magnitude. Regarding the spacecraft case study, the analysis yields a good approximation for the connection diameters of 5 and 2 mm. For the connection diameter of 1 mm, the model yields a slower process and the distance between the model and experimental curves is significant. The slower process is due to the fact that the pressure does not change along the x-axis, i.e., the model assumes that the whole tank is at the same pressure.

D. Overall comparison

To validate the curves obtained from the two-dimensional and analytical model, Figure 12, Figure13 and Figure 14 show the pressure of both tanks, for the spacecraft case study. The experimental pressure curve of the steel tank includes the sensors uncertainty.

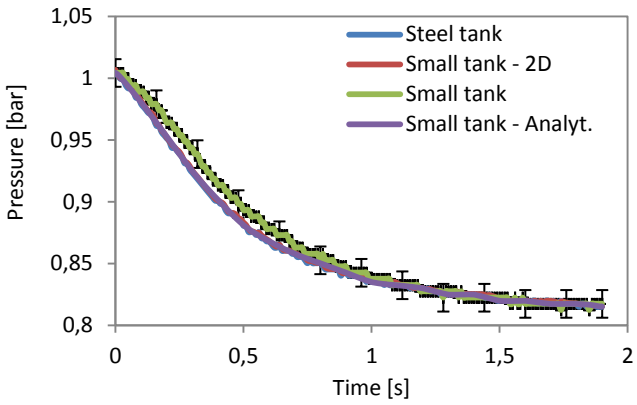

Figure 12 - Validation of the two-dimensional and analytical model for the 5 mm nozzle.

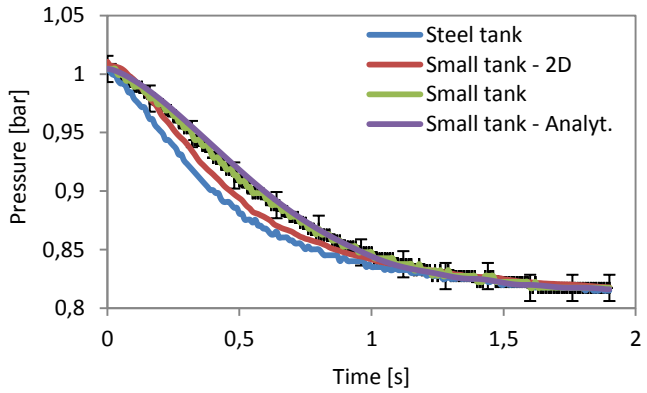

Figure 13 - Validation of the two-dimensional and analytical model for the 2 mm nozzle.

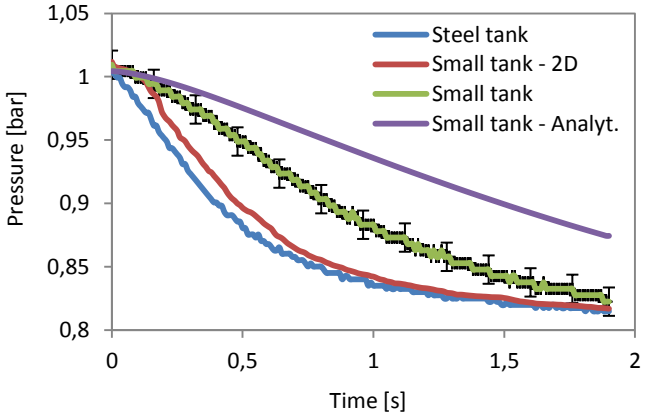

Figure 14 - Validation of the two-dimensional and analytical models for the 1 mm nozzle.

For the 5 and 2 mm nozzle, the majority of points from both curves are validated. For the 1 mm nozzle, both models present a significant distance from the experimental data.

However, the experiment is based on several approaches. For the spacecraft case study, each tank only has one sensor. On the smaller tank, the sensor is measuring the pressure close to its base. Then, the average compartment pressure is slightly smaller than the pressure recorded. Additionally, the flow from the small tank will increase the steel tank pressure. If the small tank discharges air to decrease its pressure from 1 to 0.5 bar, the steel tank pressure will increase 0.032 bar. The pressure differential between both tanks is slightly smaller which leads to a slower pressure decay rate. All the tube connections and hoses also lead to head losses, which increase as the venting area decreases. Finally, all issues mentioned above

indicate that the real pressure curves of the small tank are below the curves sketched in Figure 12, Figure13 and Figure 14.
For the present case study and considering that the real pressure curves of the smaller tank are below the curves sketched in the results above, the two-dimensional model provides a better approximation than the analytical model. In the opposite, for the compressed tank case study, the analytical analysis provides a better approximation.

VI. CONCLUSIONS

The main objective of this work was to develop a model to forecast the compartment pressure during the launch of space-vehicles. This paper also provides an one and two-dimensional numerical analysis. To validate the developed methods, a laboratory experiment was performed. The methods were applied to two different case studies. Through the results obtained, we conclude that the one-dimensional model is not suitable for both case studies, as it provides extremely fast processes. The two-dimensional model is not suitable for the compressed tank case study, but provides a useful approximation on the spacecraft case study. The analytical model provides an useful approximation for the compressed tank case study, as the times required to resettle atmospheric conditions have the same order of magnitude as the results recorded from the laboratory experiment. The model also provides an approximation for the spacecraft case study.
The main contribution of the present work is the developed analytical model, which yields the compartment pressure over time. Additionally, pressure differential between the walls of the compartment, during the launch stage, can be easily calculated. Contrarily to the developed methods described in [6], the developed analytical model does not assume an isothermal process and it is a second order differential equation.

REFERENCES

[1] Siddiqi, A. (2008) Sputnik 50 years later: New evidence on its origins, Acta Astronautica 63 (2008) 529-539, Fordham University, New York, USA.

[2] Francisco, J. (1970) NASA Space Vehicle Design Criteria, Compartment Venting, NASA SP-8060, Nov. 1970.

[3] Goldmeer, J., Urban D. and Tien, J. (1995) Effect on pressure on a burning solid in low-gravity, Conference Paper, 6 p., NASA N96-15572.

[4] Scialdone, J. (1998) Spacecraft compartment venting, Vol. 4327, p.23, San Diego, California, Technical Memorandum, NASA.

[5] Moran, M. and Shapiro H. (2009) Fundamentals of Engineering Thermodynamics, Fifth Edition, John Wiley & Sons, Inc.

[6] Benavente, F. (2015) Thermodynamic study of compartment venting, MSc thesis, Instituto Superior Técnico, Lisbon.

[7] Thomas, J. (1995) Numerical Partial Differential Equations: Finite Difference Methods, Vol. 22, Springer-Verlag New York.